Marine Biology (2000) 137: 71–85

A. Wieland · M. Kühl

Irradiance and temperature regulation of oxygenic photosynthesis and O_2 consumption in a hypersaline cyanobacterial mat (Solar Lake, Egypt)

Received: 30 November 1999 / Accepted: 11 April 2000

Abstract Short-term effects of temperature and irradiance on oxygenic photosynthesis and O_2 consumption in a hypersaline cyanobacterial mat were investigated with O_2 microsensors in a laboratory. The effect of temperature on O_2 fluxes across the mat–water interface was studied in the dark and at a saturating high surface irradiance (2162 μmol photons m^{-2} s^{-1}) in the temperature range from 15 to 45 °C. Areal rates of dark O_2 consumption increased almost linearly with temperature. The apparent activation energy of 18 kJ mol^{-1} and the corresponding Q_{10} value (25 to 35 °C) of 1.3 indicated a relative low temperature dependence of dark O_2 consumption due to mass transfer limitations imposed by the diffusive boundary layer at all temperatures. Areal rates of net photosynthesis increased with temperature up to 40 °C and exhibited a Q_{10} value (20 to 30 °C) of 2.8. Both O_2 dynamics and rates of gross photosynthesis at the mat surface increased with temperature up to 40 °C, with the most pronounced increase of gross photosynthesis at the mat surface between 25 and 35 °C (Q_{10} of 3.1). In another mat sample, measurements at increasing surface irradiances (0 to 2319 μmol photons m^{-2} s^{-1}) were performed at 25, 33 (the in situ temperature) and 40 °C. At all temperatures, areal rates of gross photosynthesis saturated with no significant reduction due to photoinhibition at high irradiances. The initial slope and the onset of saturation (E_k = 148 to 185 μmol photons m^{-2} s^{-1}) estimated from P versus E_d curves showed no clear trend with temperature, while maximal photosynthesis increased with temperature. Gross photosynthesis was stimulated by temperature at each irradiance except at the lowest irradiance of 54 μmol photons m^{-2} s^{-1}, where oxygenic gross photosynthesis and also the thickness of the photic zone was significantly reduced at 40 °C. The compensation irradiance increased with temperature, from 32 μmol photons m^{-2} s^{-1} at 25 °C to 77 μmol photons m^{-2} s^{-1} at 40 °C, due to increased rates of O_2 consumption relative to gross photosynthesis. Areal rates of O_2 consumption in the illuminated mat were higher than dark O_2 consumption at corresponding temperatures, due to an increasing O_2 consumption in the photic zone with increasing irradiance. Both light and temperature enhanced the internal O_2 cycling within hypersaline cyanobacterial mats.

Communicated by L. Hagerman, Helsingør

A. Wieland
Max-Planck-Institute for Marine Microbiology,
Microsensor Research Group,
Celsiusstr. 1, 28359 Bremen, Germany

M. Kühl · A. Wieland (✉)
Marine Biological Laboratory, University of Copenhagen,
Strandpromenaden 5, 3000 Helsingør, Denmark
e-mail: mblaw@get2net.dk

Introduction

Temperature and light are major environmental factors controlling benthic primary productivity (Cadée and Hegeman 1974; Rasmussen et al. 1983; Grant 1986; Canfield and Des Marais 1993; Barranguet et al. 1998). Benthic phototrophic communities often experience fluctuating environmental conditions, e.g. variation of the light regime as well as temperature changes, both on a daily and on a seasonal scale. During a seasonal cycle, the benthic community may acclimate and/or undergo a change in structure and composition due to such environmental fluctuations (Grant 1986; Blanchard et al. 1996; Barranguet et al. 1998).

In microbial mats photosynthesis and heterotrophic processes occur in close association within a several-millimeter-thick microbial community (van Gemerden 1993). If environmental conditions, like elevated salinities or temperature, preclude survival of higher organisms and, consequently, reduce the grazing pressure on the microbes, thick laminated microbial mats develop, which are characterized by high microbial population densities and steep physico-chemical gradients (Stal and Caumette 1994). This process can also be artificially

induced in normal coastal sediments by removal of grazing organisms (Fenchel 1998). Due to the absence of bioturbation and their compacted microbial composition, microbial mats are ideal model systems to study the regulation and interaction of numerous autotrophic and heterotrophic processes.

The required spatial resolution and sensitivity to study microbial processes on a microscale can be obtained by the application of microsensors (Revsbech and Jørgensen 1986; Amann and Kühl 1998). With the so-called light–dark shift technique the distribution of oxygenic gross photosynthesis can be determined at high spatial resolution (Revsbech and Jørgensen 1983). From depth-integrated rates of gross photosynthesis and oxygen fluxes, determined from steady-state oxygen microprofiles, oxygen consumption in the light can be estimated for distinct layers of the community, i.e. in the photic and aphotic parts of the oxic zone (Jensen and Revsbech 1989; Kühl et al. 1996).

A stimulation of oxygen consumption in the light has been demonstrated in biofilms and microbial mats (Kuenen et al. 1986; Jensen and Revsbech 1989; Neely and Wetzel 1995; Epping and Jørgensen 1996; Kühl et al. 1996) and a close coupling between oxygen- and inorganic carbon-producing/consuming processes and, therefore, between autotrophic and heterotrophic microbes was suggested (Canfield and Des Marais 1993; Kühl et al. 1996). The response of photosynthesis to light and temperature may thus also affect various heterotrophic processes in microbial mats and vice versa. Photosynthesis is strongly regulated by light, and the effect of temperature on photosynthesis seems also dependent on the light level (Davison 1991). Thus, in the natural habitat several environmental parameters vary simultaneously and determine a complex regulation of phototrophic and oxygen-consuming processes.

Solar Lake is a small hypersaline lake situated on the coast of Sinai (Egypt). The lake has a characteristic limnological cycle, with inverse thermal stratification during winter and holomixis during summer, causing pronounced variations of environmental conditions (Cohen et al. 1977). The cyanobacterial mats covering the bottom of the lake (Krumbein et al. 1977; Jørgensen et al. 1983) are characterized by steep chemical gradients as a result of the high activity of phototrophic and heterotrophic processes within the mats (Revsbech et al. 1983). Cyanobacterial mats in the shallow part of the lake are subjected to diel temperature variations (Jørgensen et al. 1979; Revsbech et al. 1983). As already indicated in earlier studies of hypersaline microbial mats from different localities (Canfield and Des Marais 1993; E.H.G. Epping and M. Kühl, unpublished results), the oxygen metabolism in the mat may be significantly regulated by both temperature and irradiance.

The aim of the present study was to obtain detailed information about the regulation of oxygenic photosynthesis and O_2-consuming processes by temperature and irradiance. We studied the short-term response of oxygenic photosynthesis and O_2 consumption to varying light and temperature conditions in a Solar Lake cyanobacterial mat by use of O_2 microsensors under controlled laboratory conditions. In another study, we also investigated the interactions of O_2- and H_2S-producing/consuming processes in microbial mats and how these are regulated by temperature under dark and light conditions (Wieland and Kühl 2000).

Materials and methods

Samples

Microbial mats were collected in the shallow eastern part of the hypersaline Solar Lake (Sinai, Egypt) at an approximate water depth of 0.4 to 0.5 m in June 1997. The mat samples (3 to 4 cm thick) were taken by Plexiglas corers with an inner diameter of 5.0 to 5.6 cm. The in situ temperature was 33 °C and the salinity at the sampling site was 114‰, as determined by a refractometer (Atago, Japan). Maximal irradiances at noon reached ~2300 μmol photons m^{-2} s^{-1} (Eilat, Israel). The mat samples in the cores were transported to the Interuniversity Institute in Eilat within a few hours after sampling, where measurements were performed under controlled laboratory conditions.

Experimental set-up

Mat subsamples (approximately $2.5 \times 2.5 \times 2$ cm) were immobilized [1.5% agar (w/v) in filtered Solar Lake water] and mounted in a flow chamber modified from Lorenzen et al. (1995). The flow chamber was connected to a submersible water pump (E-Heim, Germany), which created a constant flow of aerated and filtered Solar Lake water over the mat surface. Experimental temperatures of the water reservoir were adjusted to ± 0.5 °C with a heat-exchanging metal coil connected to a thermostat (Julabo, Germany). The mat surface was illuminated with a fiber-optic halogen light source (Schott KL 1500, Germany). Neutral density filters (Oriel, USA) were inserted in the collimated light beam to adjust the downwelling surface irradiance, E_d (PAR). For quantification of E_d (PAR) with an underwater quantum irradiance meter (LiCor, USA), the flow chamber was replaced by the underwater quantum sensor, which was submerged in Solar Lake water and placed at the same position and distance as the mat sample relative to the light source.

Microsensor measurements

Microprofiles of O_2 and gross photosynthesis were measured with Clark-type O_2 microelectrodes (Revsbech 1989). The O_2 microelectrodes had outer tip diameters of < 10 μm, stirring sensitivities of $< 2\%$ and t_{90} response times of < 0.5 s. The O_2 microelectrodes were connected to a fast-responding, miniaturized picoammeter (MasCom GmbH, Germany) plugged into the prolonged shaft of the microelectrodes and mounted on a motor-driven micromanipulator (Oriel, USA; Märzhäuser, Germany). The microsensors were positioned on the mat surface by use of the micromanipulator, while watching the mat surface and the tip of the microelectrode through a dissection microscope (Zeiss, Germany). The measuring signals were recorded on a strip chart recorder (Servogor, UK) and on the computer data acquisition system (National Instruments, Labview, USA) that also controlled the micromanipulator. Linear calibration of the O_2 microelectrode from readings in the aerated overlying Solar Lake water (100% air saturation) and in the anoxic part of the mat (0% oxygen) was done with every measured profile. Dissolved O_2 concentrations in aerated Solar Lake brine at experimental temperatures and salinities were calculated according to Sherwood et al. (1991). Steady-state O_2 microprofiles were measured in intervals of 100 μm vertical depth.

Gross photosynthesis was measured by means of the light–dark shift technique (Revsbech and Jørgensen 1983). The mat surface was darkened by closing an electronic shutter (Vincent Ass., Uniblitz, USA), which was fixed in the light beam and triggered by the data acquisition software. A photodiode close to the shutter registered the moment of darkening. The rate of O_2 depletion after darkening of the mat was calculated automatically via linear regression over the initial 1 to 2 s by the software. Gross photosynthesis profiles were recorded with a resolution of 100 µm vertical depth. Since volumetric gross photosynthetic rates determined with the light–dark shift technique are given as nanomoles of O_2 per cubic centimeter (porewater) per second (Revsbech et al. 1981), measured rates of volumetric gross photosynthesis were corrected for porosity, which was assumed to be 0.9 (Jørgensen and Cohen 1977; Jørgensen et al. 1979). Gross photosynthesis rates measured with the light–dark shift microsensor technique seem to include O_2 consumed by photorespiration but not by the Mehler reaction, since the latter is tightly coupled to light-dependent photosynthetic electron transport, whereas photorespiration continues for several seconds after light is extinguished (Glud et al. 1992). The zone where gross photosynthesis was measurable with the light–dark shift technique is hereafter referred to as the photic zone. The aphotic zone represents the oxic zone below the photic zone.

Experimental light–dark cycles at increasing temperatures were performed on the mat surface at a downwelling irradiance of 2162 µmol photons m^{-2} s^{-1}. The O_2 microelectrode was positioned on the mat surface, and after reaching O_2 steady-state levels in the dark (light), the light was turned on (off).

Calculations

Diffusive fluxes of O_2 across the mat–water interface, J_o, were calculated from steady-state O_2 profiles using Fick's first law of (one-dimensional) diffusion:

$$J_o = -D_o \left[\frac{dC(z)}{dz}\right] , \quad (1)$$

where D_o is the free solution molecular diffusion coefficient of O_2, and $\{[dC(z)]/dz\}$ is the linear O_2 concentration gradient in the diffusive boundary layer above the mat surface, where transport of solutes is dominated by molecular diffusion (Jørgensen and Revsbech 1985). A positive flux indicates a net O_2 uptake, while a negative flux indicates a net O_2 export out of the mat. In the dark-incubated mat, J_o is a measure of O_2 consumption rate per unit area of the microbial mat, R_{dark}. In the light-incubated mat, $-J_o$ is a measure of areal rates of net photosynthesis, P_n. If O_2 consumption is higher than gross photosynthesis, this leads to a net O_2 uptake in the light and P_n is, therefore, negative. Areal rates of net photosynthesis in the photic zone, $P_{n,phot}$, were calculated as the total O_2 flux out of the photic zone (Jensen and Revsbech 1989; Kühl et al. 1996):

$$P_{n,phot} = J_s - J_o . \quad (2)$$

The downward O_2 flux, J_s, at the lower boundary of the photic zone, which is also a measure of O_2 consumption in the aphotic zone, R_{aphot}, was calculated by:

$$J_s = -\phi\, D_s \left[\frac{dC(z)}{dz}\right] . \quad (3)$$

The porosity, ϕ, of the mat was assumed to be 0.9 (see above). The sediment diffusion coefficient, D_s, was calculated from the mat porosity and the free solution molecular diffusion coefficient, D_o, according to Ullman and Aller (1982):

$$D_s = \phi^2\, D_o . \quad (4)$$

The free solution molecular diffusion coefficient of O_2 was taken from Broecker and Peng (1974) and corrected for temperature and salinity (Li and Gregory 1974).

Areal rates of total O_2 consumption in the light, R_{light}, and of O_2 consumption in the photic zone, R_{phot}, were calculated by (Canfield and Des Marais 1993; Kühl et al. 1996):

$$R_{light} = P_g - P_n \quad \text{and} \quad (5)$$

$$R_{phot} = P_g - P_{n,phot} , \quad (6)$$

where P_g is the areal rate of gross photosynthesis, calculated by integration of the porosity corrected volumetric gross photosynthesis rates over the depth of the photic zone. Volumetric rates of O_2 consumption in the photic zone were calculated by dividing calculated areal rates of R_{phot} (Eq. 6) by the thickness of the photic zone.

Photosynthesis versus irradiance curves (P vs E_d curves) were obtained by fitting areal rates of gross photosynthesis at increasing irradiances to an exponential function (Webb et al. 1974) using the solver routine of Excel 5.0 (Microsoft):

$$P = P_m \left[1 - \exp\left(\frac{-\alpha E_d}{P_m}\right)\right] , \quad (7)$$

where P_m is the maximal photosynthetic rate at light saturation, and α is the initial slope of the P versus E_d curve.

The effect of temperature on process rates was quantified by calculating the apparent activation energy, E_a, and the corresponding Q_{10} according to Isaksen and Jørgensen (1996). E_a was determined from the slope of an Arrhenius plot, i.e. $\ln(k)$ versus $(R\ T)^{-1}$, based on the integrated form of the Arrhenius equation:

$$\ln(k) = \ln(A) + [-E_a\ (R\ T)^{-1}] , \quad (8)$$

where k is the process rate, A is the Arrhenius constant, R is the gas constant (8.3144 J K^{-1} mol^{-1}) and T is the absolute temperature (K). Q_{10}, which is the factor of process rate increase by a 10 °C temperature increase, was calculated by:

$$Q_{10} = \exp\{E_a\ 10\text{K}\ [R\ T\ (T + 10\text{K})]^{-1}\} . \quad (9)$$

Results

Structure

The microbial mat had a gelatinous structure with a 1 to 2 mm thick yellow-brownish surface layer composed of diatoms (*Navicula* sp., *Nitzschia* sp.) and unicellular cyanobacteria, belonging to the *Halothece* cluster (Garcia-Pichel et al. 1998). The surface layer was followed by a dense ca. 0.5 to 1 mm thick green layer of filamentous cyanobacteria (mainly *Microcoleus chthonoplastes*). At higher experimental temperatures, the mat topography became rough, probably due to migration and aggregation of microbes in the surface layer of the mat.

Oxygen fluxes as a function of temperature

In the dark-incubated mat, O_2 penetration and O_2 concentration at the mat surface decreased gradually from 15 to 35 °C. At further increasing temperatures, the O_2 concentration at the mat surface slightly increased again (Fig. 1). In the light-incubated mat [E_d (PAR): 2162 µmol photons m^{-2} s^{-1}], O_2 penetration decreased from 3.8 mm at 15 °C to 2.1 mm at 35 °C, and did not change significantly at 40 or 45 °C (profiles not shown).

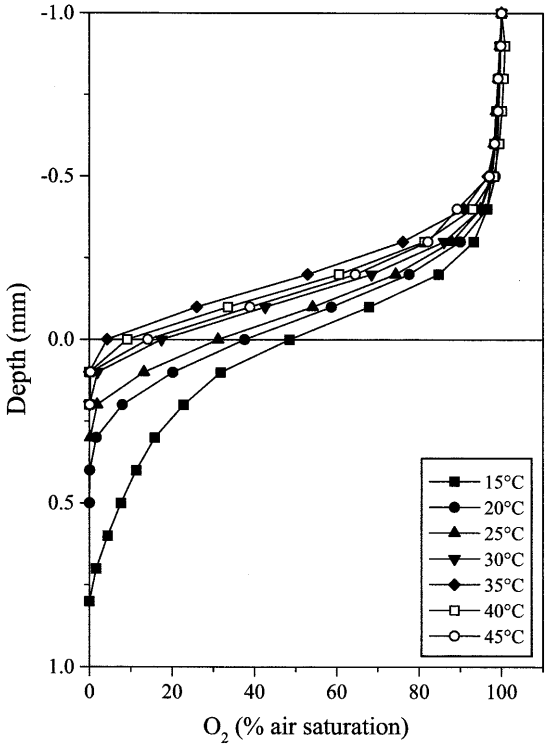

Fig. 1 Averaged steady-state O_2 concentration profiles (n = 3) measured in a dark-incubated mat at increasing temperatures (see figure key). Note that the 100% air saturation value translates into decreasing amounts of absolute O_2 concentration with increasing temperature

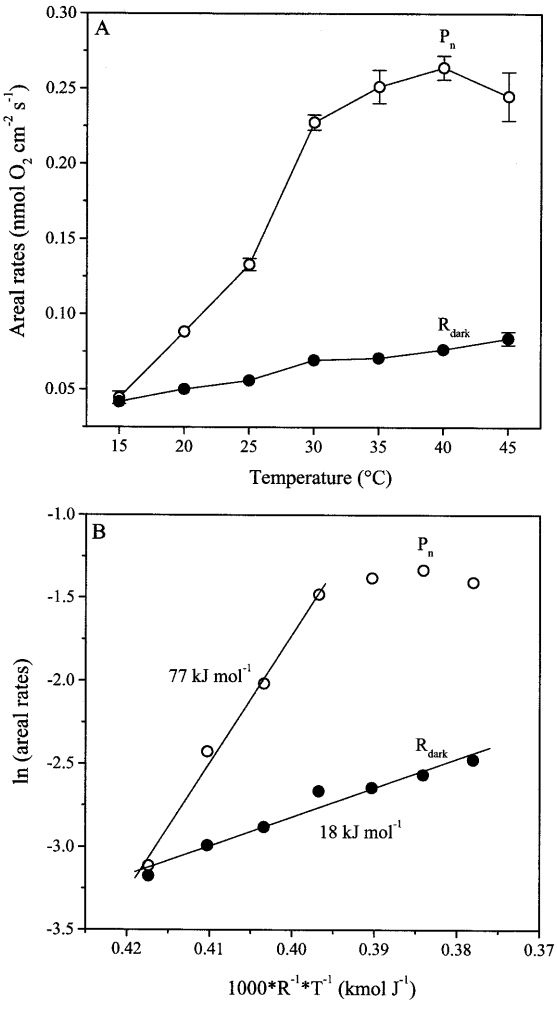

Fig. 2 **A** Areal rates of dark O_2 consumption, R_{dark}, and of net photosynthesis, P_n, at increasing temperatures. Symbol and error bars indicate mean ± standard deviation (n = 2 to 3). **B** Arrhenius plot of the rates shown in **A**

Areal rates of dark O_2 consumption, R_{dark}, increased almost linearly with temperature from 0.042 (±0.001) nmol O_2 cm^{-2} s^{-1} at 15 °C to 0.084 (±0.004) nmol O_2 cm^{-2} s^{-1} at 45 °C (Fig. 2A). The apparent activation energy of R_{dark}, as determined from the linear slope of an Arrhenius plot of these data, amounted to 18 kJ mol^{-1} (Fig. 2B) and is a measure of the temperature response of all O_2-consuming processes in the mat. In the light-incubated mat [E_d (PAR): 2162 µmol photons m^{-2} s^{-1}], areal rates of net photosynthesis, P_n, increased between 15 and 40 °C from 0.044 (±0.004) to 0.264 (±0.008) nmol O_2 cm^{-2} s^{-1}, and then slightly decreased at 45 °C to 0.245 (±0.016) nmol O_2 cm^{-2} s^{-1} (Fig. 2A). The apparent activation energy, calculated in the temperature range from 15 to 30 °C, amounted to 77 kJ mol^{-1} (Fig. 2B). From the activation energies, we calculated Q_{10} values of 1.3 (25 to 35 °C) and 2.8 (20 to 30 °C) for areal dark O_2 consumption and net photosynthesis, respectively.

Oxygen dynamics at the mat surface as a function of temperature

Both the steady-state O_2 levels and the O_2 dynamics at the mat surface changed with increasing temperature (Fig. 3). The O_2 steady-state concentration in the light increased from 283 µ*M* at 15 °C to 596 µ*M* at 40 °C, whereas the O_2 steady-state concentration in the dark decreased from 93 µ*M* at 15 °C to 10 µ*M* at 40 °C. The initial rate of O_2 depletion after darkening, i.e. the gross photosynthesis at the mat surface, increased with temperature up to 40 °C and then decreased at 45 °C (Fig. 4A). An apparent activation energy of 86 kJ mol^{-1} in the temperature range from 15 to 35 °C was calculated (Fig. 4B), yielding a Q_{10} of 3.1 (25 to 35 °C).

Microprofiles of O_2 and gross photosynthesis

In another mat subsample, depth profiles of dissolved O_2 and gross photosynthesis were measured as a function of increasing downwelling irradiance and temperature (Fig. 5). At all experimental temperatures, O_2 penetration increased with increasing irradiance. Oxygen concentrations within the mat increased with irradiance up to a maximal O_2 concentration at 626 µmol photons m^{-2} s^{-1} at each experimental temperature. Oxygen penetration in the dark decreased with increasing temperature from

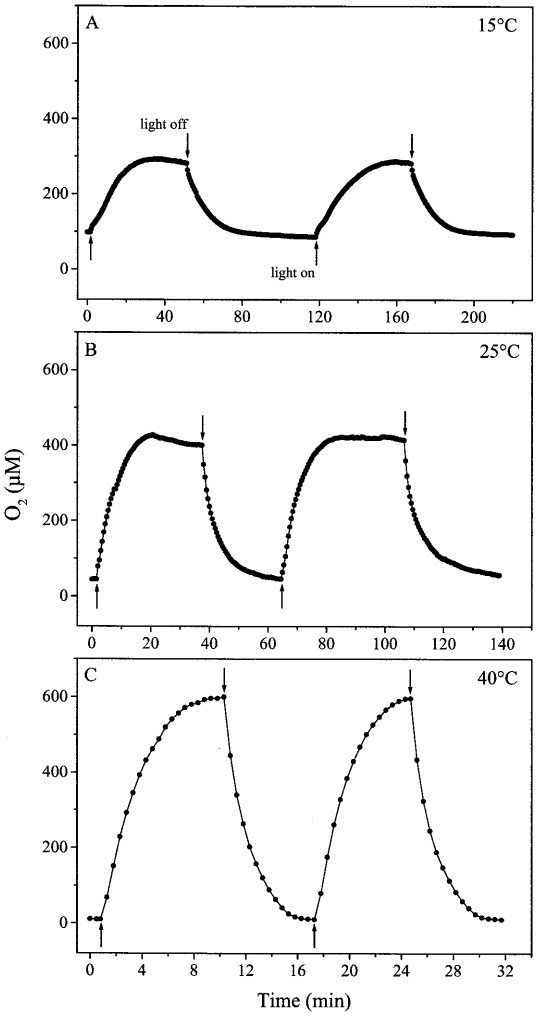

Fig. 3 Oxygen dynamics at the mat surface during experimental light–dark cycles [E_d (PAR): 2162 µmol photons m^{-2} s^{-1}] at **A** 15 °C, **B** 25 °C and **C** 40 °C. Note different time scales

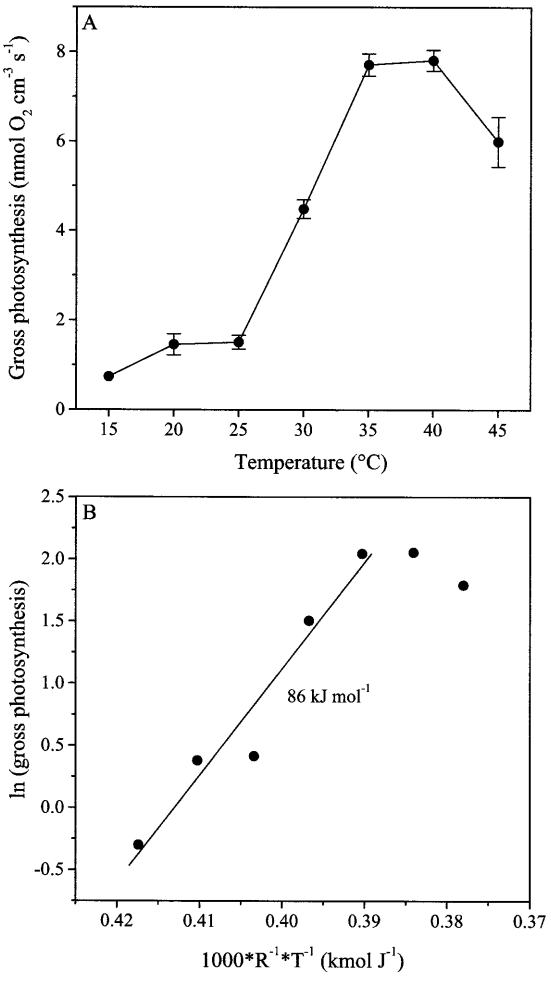

Fig. 4 **A** The initial rate of O_2 depletion after darkening, i.e. gross photosynthesis, as determined at the mat surface from experimental light–dark cycles at increasing temperatures (calculated from data in Fig. 3). Symbols and error bars indicate mean ± standard deviation (n = 2 to 3). **B** Arrhenius plot of the rates shown in **A**

0.5 mm at 25 °C to 0.2 mm at 40 °C. A temperature-induced decrease of O_2 penetration was also found in the illuminated mat. At low irradiances of 54 and 119 µmol photons m^{-2} s^{-1}, both O_2 penetration and peak O_2 concentration decreased with temperature. At 54 µmol photons m^{-2} s^{-1}, a gradual, temperature-dependent transition from a net O_2 export (25 °C) towards a net O_2 import (40 °C) across the mat–water interface was observed. Peak O_2 concentrations at high irradiances, i.e. 626, 1000 and 2319 µmol photons m^{-2} s^{-1}, were maximal at 25 °C and minimal at 33 °C at each irradiance. The thickness of the aphotic zone decreased under each light condition with increasing temperature.

The vertical zonation of gross photosynthetic activity changed with increasing irradiance and exhibited two to three distinct zones of high activity at saturating irradiances. At low irradiances, the thickness of the photic zone was constant at 25 °C (1.7 mm) and 33 °C (1.5 mm), whereas at 40 °C it increased significantly from 0.7 to 1.6 mm between 54 and 119 µmol photons m^{-2} s^{-1}. At each temperature, an additional subsurface peak of photosynthesis was found at 626 µmol photons m^{-2} s^{-1}. This peak moved deeper into the mat at higher irradiance (Figs. 5, 6C).

At each temperature, the volumetric gross photosynthesis rate at the mat surface increased with irradiance up to 626 µmol photons m^{-2} s^{-1}, and decreased at higher irradiances (Fig. 6A). The averaged volumetric gross photosynthesis rate in the upper 0.1 to 0.7 mm of the mat showed a similar trend at 33 and 40 °C (Fig. 6B). At 25 °C, the averaged gross photosynthesis rate did not decrease, but approached saturation at high irradiances.

Photosynthesis versus irradiance at three experimental temperatures

At each temperature, areal rates of gross photosynthesis, P_g, increased with irradiance up to 626 µmol photons m^{-2} s^{-1} (Fig. 7, left panels). The initial slope of the P

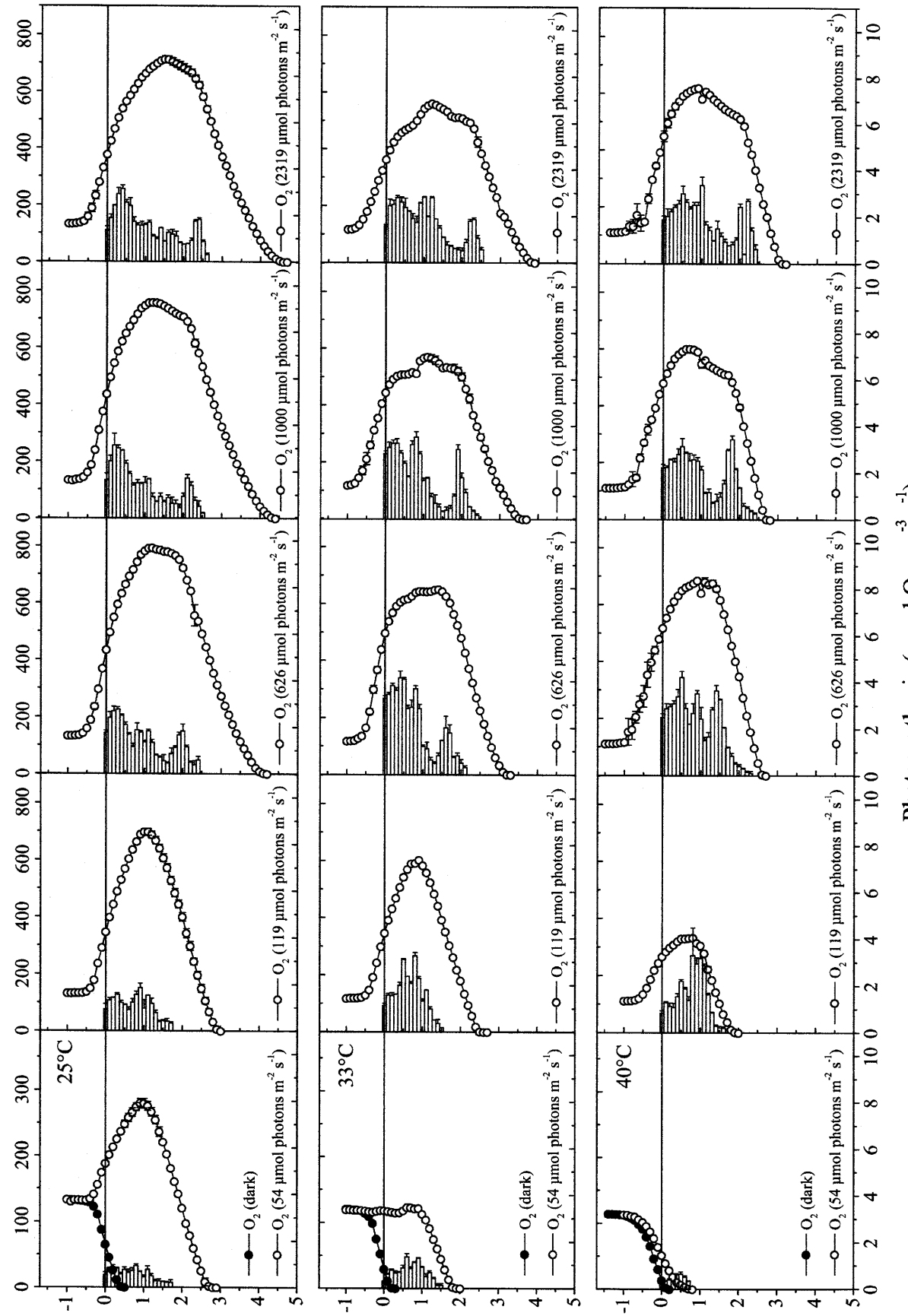
25°C
33°C
40°C
O2 (dark)
O2 (54 µmol photons m-2 s-1)
O2 (119 µmol photons m-2 s-1)
O2 (626 µmol photons m-2 s-1)
O2 (1000 µmol photons m-2 s-1)
O2 (2319 µmol photons m-2 s-1)
O2 (µM)
Depth (mm)
Photosynthesis (nmol O2 cm-3 s-1)

◀

Fig. 5 Averaged depth profiles of O_2 concentration and gross photosynthesis as a function of increasing downwelling irradiance at 25 °C (*upper panels*), 33 °C (*central panels*), and 40 °C (*lower panels*). Note the different O_2 concentration scales. Standard deviation of gross photosynthesis at each depth is indicated by error bars (n = 2 to 5). Error bars were only included in the averaged O_2 profiles (n = 2 to 3) if the standard deviation was higher than the O_2 concentration range that is comprised by the symbol

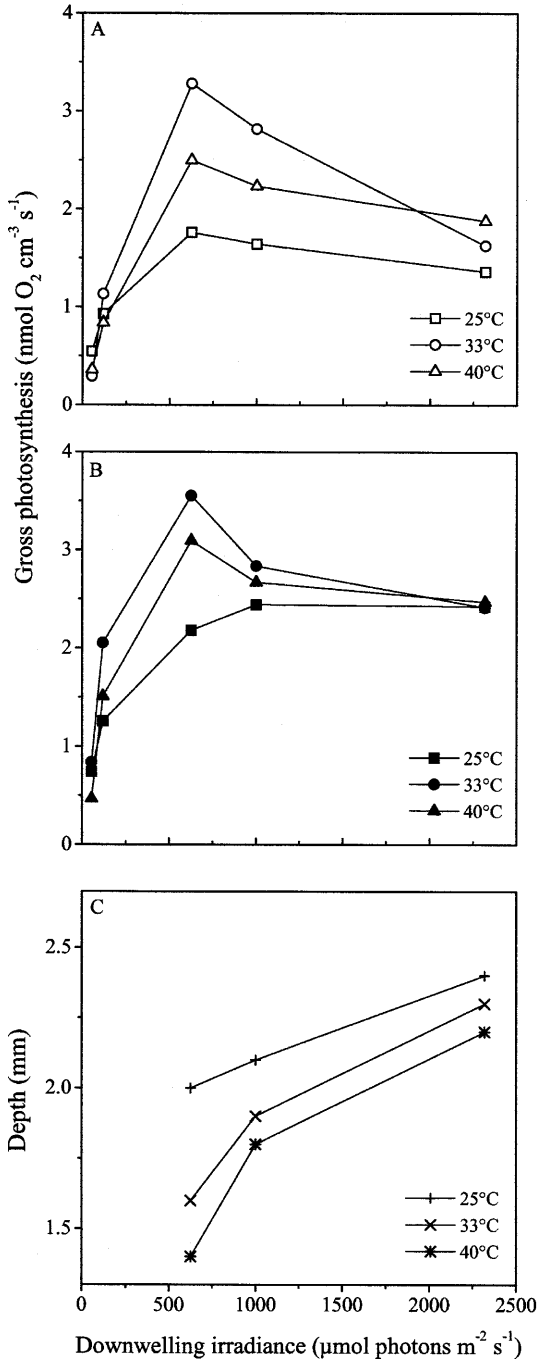

Fig. 6 **A** Volumetric gross photosynthesis rate at the mat surface, **B** the averaged volumetric gross photosynthesis rate in the upper 0.1 to 0.7 mm of the mat, and **C** the depth of the maximal volumetric gross photosynthesis rate of the subsurface photosynthesis peak versus downwelling irradiance at 25, 33 and 40 °C

versus E_d curve, α, and the onset of saturation at irradiance $E_k = P_m/\alpha$ showed no clear trend with temperature and amounted to α = 0.0022, 0.0031 and 0.0026, and to E_k = 175, 148 and 185 µmol photons m^{-2} s^{-1} at 25, 33 and 40 °C, respectively. The maximal photosynthetic rate at light saturation, P_m (Eq. 7), increased from 0.38 nmol O_2 cm^{-2} s^{-1} at 25 °C to 0.48 nmol O_2 cm^{-2} s^{-1}at 40 °C. An increase of P_g with temperature was found at each irradiance except at 54 µmol photons m^{-2} s^{-1}, where P_g first increased between 25 and 33 °C, and then decreased again at 40 °C.

Areal rates of net photosynthesis, P_n, and of net photosynthesis in the photic zone, $P_{n,phot}$, increased with irradiance up to 626 µmol photons m^{-2} s^{-1} at each temperature and then either decreased (25 and 33 °C) or further increased with increasing irradiance (40 °C). The compensation irradiance, E_c, where O_2 production (P_g) is balanced by O_2 consumption (R_{light}), i.e. P_n = 0, increased with temperature from 32 µmol photons m^{-2} s^{-1} at 25 °C to 53 µmol photons m^{-2} s^{-1} at 33 °C and to 77 µmol photons m^{-2} s^{-1} at 40 °C.

Oxygen consumption versus irradiance at three experimental temperatures

From the measured gross photosynthesis rates and the O_2 fluxes determined from the measured O_2 profiles (Fig. 5), rates of O_2 consumption were calculated (see "Materials and methods"). Areal rates of total O_2 consumption in the mat, R_{light}, increased at each temperature with irradiance up to 626 µmol photons m^{-2} s^{-1} (Fig. 7, right panels). At higher irradiances, R_{light} increased further (25 °C) or approached saturation (33 °C), while at 40 °C R_{light} decreased at irradiances above 626 µmol photons m^{-2} s^{-1}. Areal rates of O_2 consumption in the photic zone, R_{phot}, showed in general a similar trend, but decreased between 54 and 119 µmol photons m^{-2} s^{-1}at 25 and 33 °C. Rates of O_2 consumption in the aphotic zone, R_{aphot}, initially increased with irradiance at each temperature, but were almost invariant at high irradiances as compared to R_{light} and R_{phot}. At high irradiances, R_{phot} was always higher than R_{aphot} and thus mainly contributed to R_{light}.

At each temperature, both R_{light} and R_{phot} increased with P_g until gross photosynthesis was saturated (Fig. 8). R_{aphot} showed a less pronounced correlation with gross photosynthesis.

Effect of temperature and irradiance on O_2 turnover

Areal rates of dark O_2 consumption, R_{dark}, showed no clear trend with temperature (Fig. 9A). At all irradiances, R_{light} was higher than R_{dark} at corresponding temperatures. At 54 µmol photons m^{-2} s^{-1} (Fig. 9B), temperature had a significant effect on the balance between photosynthesis and O_2 consumption. Both gross photosynthesis, P_g, and total O_2 consumption, R_{light},

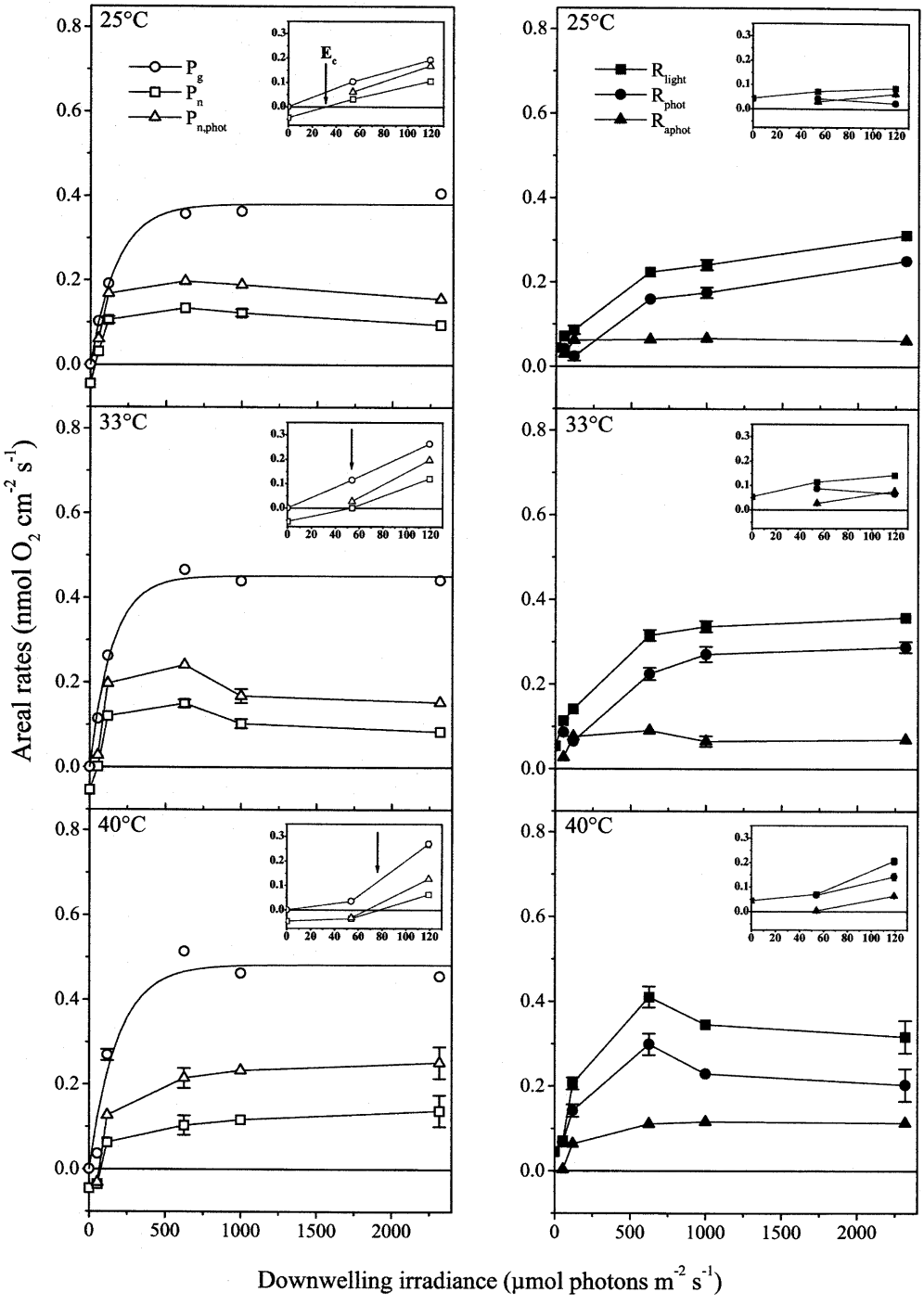

Fig. 7 Areal rates of gross photosynthesis, P_g, net photosynthesis, P_n, net photosynthesis in the photic zone, $P_{n,phot}$ (*left panels*), and areal rates of total O_2 consumption, R_{light}, O_2 consumption in the photic zone, R_{phot}, and in the aphotic zone, R_{aphot} (*right panels*), versus downwelling irradiance at 25, 33 and 40 °C. Areal rates of gross photosynthesis were fitted (*solid lines*) to an exponential function (Webb et al. 1974). Areal rates at irradiances below 120 µmol photons m^{-2} s^{-1} are shown in more detail within the graph insets

increased with temperature from 25 to 33 °C and then decreased again at 40 °C. Net photosynthesis, P_n, decreased with temperature. At 25 °C, R_{light} amounted to 70% of P_g, whereas at 33 °C photosynthetic O_2 production was almost balanced by O_2 consumption (99% of P_g). At 40 °C, O_2 consumption exceeded photosynthetic O_2 production (197% of P_g), leading to an import of O_2 across the mat–water interface, which almost equaled the O_2 supply by photosynthesis (97% of P_g). Relative to P_g, R_{phot} strongly increased with temperature from 41% at 25 °C to 187% at 40 °C. Both absolute and relative rates of R_{aphot} and P_n decreased with temperature.

At 119 and 626 µmol photons m^{-2} s^{-1} (Fig. 9C, D), P_g as well as R_{phot} and R_{light} increased with temperature. At 25 °C, 55 to 37% of the photosynthetically produced O_2 diffused out of the mat, whereas the remaining 45 to 63% was consumed within the mat. At higher temperatures, the relative O_2 export across the mat–water interface, P_n, decreased with temperature due to increased O_2 consumption within the mat. Relative to P_g, R_{aphot}

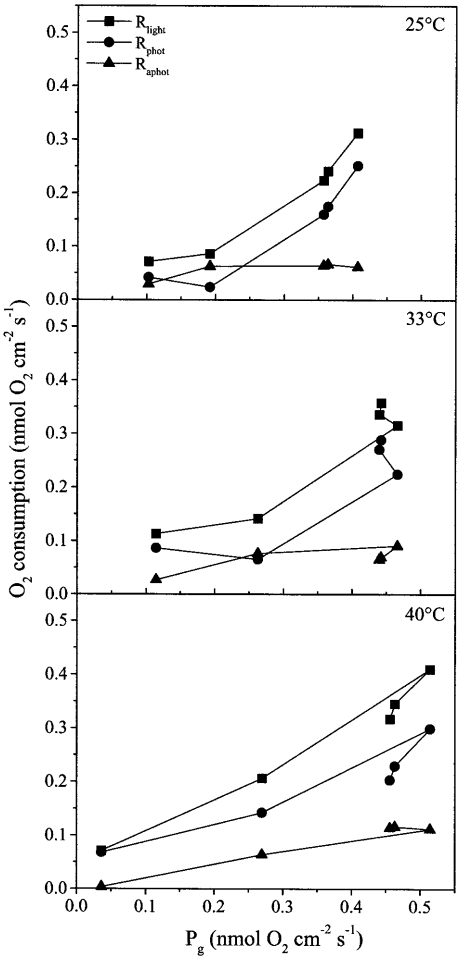

Fig. 8 Areal rates of O_2 consumption in the photic zone, R_{phot}, in the aphotic zone, R_{aphot}, and total O_2 consumption in the light-incubated mat, R_{light}, versus areal rates of gross photosynthesis, P_g, at 25, 33 and 40 °C. At each temperature, the succession of the symbols indicates the rates at increasing irradiances

decreased (119 µmol photons m^{-2} s^{-1}) or increased (626 µmol photons m^{-2} s^{-1}) with temperature.

At 1000 and 2319 µmol photons m^{-2} s^{-1} (Fig. 9E, F), similar trends were observed. However, the percentage of the produced O_2 which was consumed within the mat decreased at 40 °C. R_{aphot} increased between 33 and 40 °C. Although P_g was highest at 40 °C, R_{phot} decreased so strongly that even the increased rates of R_{aphot} could not compensate for the decrease, and thus the relative O_2 consumption within the mat decreased, resulting in an increased O_2 export across the mat–water interface, i.e. an increase of net photosynthesis.

Discussion

Temperature and diffusive boundary layer effects on O_2 fluxes

Our data showed a temperature-induced increase of the O_2 dynamics at the mat surface and of the fluxes across the mat–water interface. In highly active communities, the diffusive boundary layer (DBL) poses a mass-transfer resistance and thus limits the O_2 flux across the solid–water interface (Jørgensen and Revsbech 1985; Jørgensen and Des Marais 1990; Kühl and Jørgensen 1992a; Kühl et al. 1996). The thickness of the DBL is influenced by the hydrodynamic conditions (e.g. flow velocity) and the roughness (topography) of the mat (Jørgensen and Revsbech 1985; Jørgensen and Des Marais 1990).

Temperature increases the diffusive O_2 transport through the DBL, since the diffusion coefficient of O_2 increases, and theoretically the DBL thickness decreases with temperature (Jørgensen and Revsbech 1985). This is, however, partly counterbalanced by a decreased O_2 solubility at higher temperature. Thus, the effect of temperature on the O_2 exchange across the mat–water interface is not only determined by temperature-induced changes of biological activity, but also by temperature effects on the hydrodynamics and other physical parameters influencing the O_2 flux across the mat–water interface (see above).

The presence of a microsensor above the mat induces a local compression of the DBL (Glud et al. 1994). This effect is most pronounced for smooth surface topographies and seems to be alleviated in heterogeneous phototrophic mats (Lorenzen et al. 1995). It was concluded that the microsensor-induced DBL compression can be treated as being equivalent to measuring at a higher local flow velocity (Lorenzen et al. 1995), as long as the microsensor is kept near the mat surface for periods long enough to allow steady-state conditions to establish (Glud et al. 1994). The exact mechanism behind the DBL compression and whether it has a temperature-dependent component, e.g. due to changes in fluid viscosity and density, awaits further investigation.

In the dark-incubated mat, the O_2 flux into the mat, representing dark O_2 consumption R_{dark}, was enhanced by increasing temperatures (Fig. 2), which amounted to an increase of 102% between 15 and 45 °C. The O_2 diffusion coefficient increased by 99%, and O_2 solubility decreased by 27%. Theoretically, the effective thickness of the DBL, Z_δ, should decrease by 24% between 15 and 45 °C, as estimated by the equation for the calculation of Z_δ for flow over a flat plate (Jørgensen and Revsbech 1985; Vogel 1989):

$$Z_\delta = 5\sqrt{\frac{x\mu}{U\rho}}\ , \qquad (10)$$

where x is the distance from the leading edge of the plate, U is the flow velocity, µ is the dynamic viscosity and ρ is the density of the liquid. The theoretical decrease of Z_δ with temperature was calculated from Eq. 10, using Z_δ determined from the measured O_2 profile at 15 °C (280 µm) with the temperature-dependent changes of µ and ρ (Riley and Skirrow 1975; Millero and Poisson 1981).

With these values, we would expect an increase of the O_2 flux by 91% between 15 and 45 °C, as estimated from the equation (Jørgensen and Revsbech 1985):

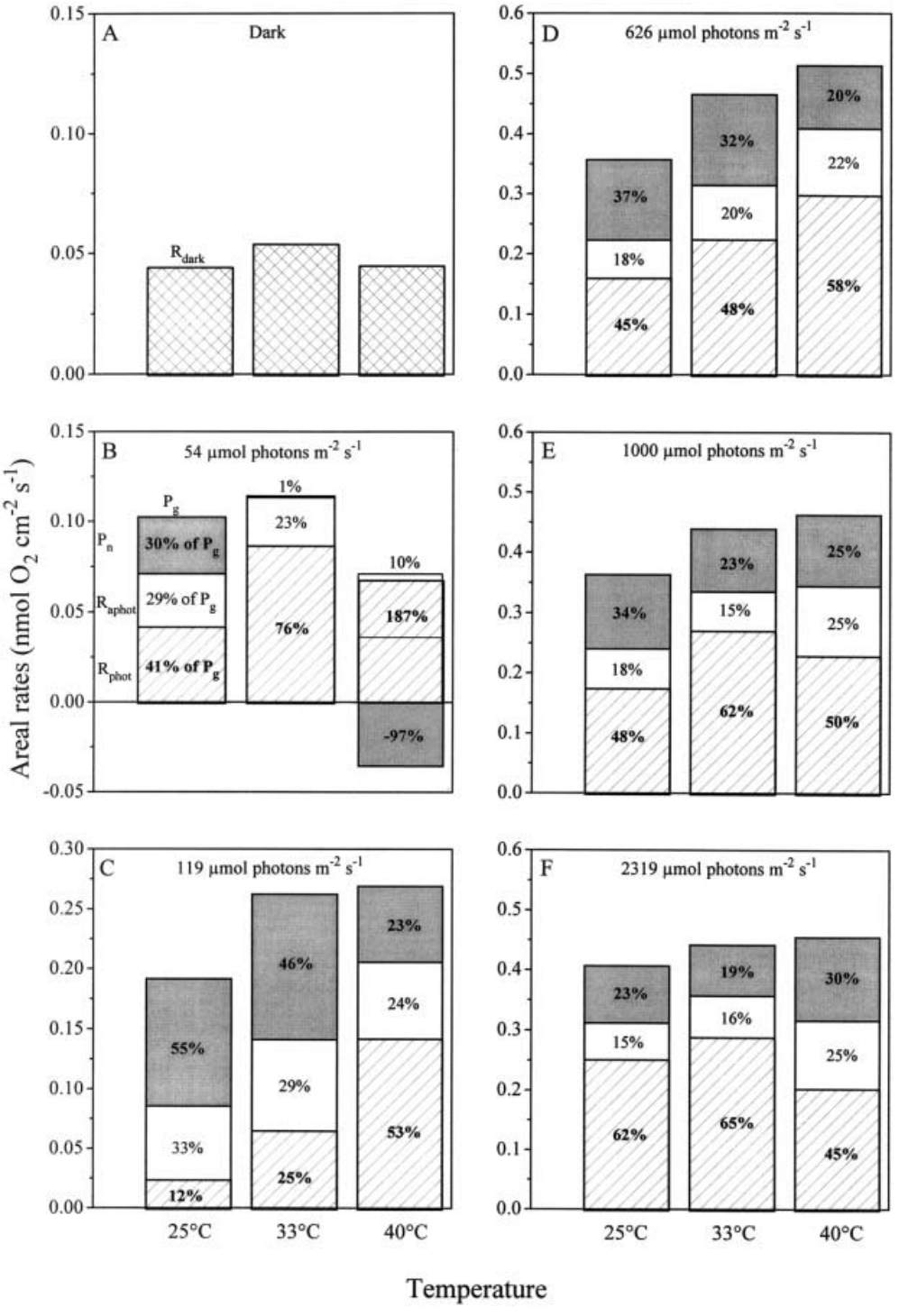

Fig. 9 **A** Areal rates of dark O_2 consumption (R_{dark}) versus temperature. Areal rates of gross photosynthesis (P_g) versus temperature at **B** 54, **C** 119, **D** 626, **E** 1000, and **F** 2319 µmol photons m^{-2} s^{-1}, respectively. Gray areas in the columns represent areal rates of net photosynthesis (P_n), white areas represent areal rates of O_2 consumption in the aphotic zone (R_{aphot}), and hatched areas in the columns represent areal rates of O_2 consumption in the photic zone (R_{phot}). Total O_2 consumption, R_{light}, is represented by the sum of R_{phot} and R_{aphot}. Areal rates of P_n, R_{phot} and R_{aphot} are also expressed relative to P_g (numbers in the corresponding zones of the columns). Note the different scales

$$J = D\ (\Delta O_2)/Z_\delta\ , \qquad (11)$$

where ΔO_2 is the difference between the O_2 concentration in the bulk water and at the mat surface, which was determined from the dark O_2 profile at 15 °C.

However, we cannot differentiate clearly between the contribution of temperature-induced changes of biological activity and of physical parameters to the measured changes of R_{dark}. As calculated from Eq. 10, Z_δ should theoretically decrease from 280 µm at 15 °C (see above) to 213 µm at 45 °C. In our data, Z_δ showed an increasing trend with temperature, as determined from measured dark O_2 profiles, and increased from 280 µm at 15 °C to 341 µm at 45 °C. This points to a temperature-dependent change in surface roughness, e.g. due to migration of microbes. Increased surface roughness tends to retard the flow and therefore leads to a thicker DBL (Jørgensen and Des Marais 1990).

We found a relatively low Q_{10} value of 1.3 for dark O_2 consumption. At elevated temperatures, enhanced O_2 consumption reduced O_2 penetration to the uppermost 0.1 to 0.2 mm of the mat (Fig. 1). Since Z_δ increased slightly with temperature, the total O_2 consumption of the mat was apparently limited by the diffusive O_2 supply through the DBL. The low temperature dependence of R_{dark} can thus be explained by the constraints on mass transfer imposed by the DBL at all experimental temperatures. Thamdrup et al. (1998) postulated that the effect of temperature on diffusive oxygen fluxes (considering only dark aerobic respiration) is reduced considerably by the diffusive constraints imposed by the DBL.

R_{dark} includes both O_2 consumption due to aerobic heterotrophic respiration and due to oxidation of reduced inorganic compounds like sulfide. Temperature stimulates both processes directly, and sulfide oxidation could have been further enhanced by an increased sulfide flux towards the mat surface, as sulfate reduction in hypersaline mats is known to increase with temperature (Skyring et al. 1983; Canfield and Des Marais 1991, 1993; Jørgensen 1994). In a separate study, we quantified the temperature-induced increase of net sulfide production/consumption rates in a Solar Lake mat sampled during the winter period (November 1996) (Wieland and Kühl 2000). In that mat, a significant stimulation of both sulfate reduction and sulfide oxidation was observed with increasing temperature, and an increasing amount of O_2 consumption at elevated temperature was due to sulfide oxidation. However, both the structure and the microbial composition of the surface layer differed from the mat investigated in the present study, and we can only speculate on the role of sulfide in the present study.

The temperature-induced changes of net photosynthesis, P_n, represent the combined effect of temperature on the mass transfer resistance imposed by the DBL, and on gross photosynthesis and O_2 consumption within the mat. Net photosynthesis at 2162 µmol photons m^{-2} s^{-1} reached an optimum at 40 °C (Fig. 2A), and was thus highest in the temperature range around the observed in situ temperature. The calculated Q_{10} of 2.8 for P_n is within the range of reported values for light-saturated photosynthesis (Davison 1991). The observed temperature-induced increase in O_2 dynamics at the mat surface (Fig. 3) can be explained by increased gross photosynthetic activity as well as by increased O_2 consumption. The temperature-enhanced rates of gross photosynthesis at the mat surface indicate that light-saturated gross photosynthesis was regulated by temperature-sensitive processes involved in carbon assimilation.

Regulation of photosynthesis by irradiance and temperature

In microbial mats and other densely populated phototrophic communities, light is strongly attenuated due to scattering and absorption by phototrophic organisms, resulting in a steep light gradient within the mat. The spectral composition of light is changing within the community due to selective absorbance of light qualities by various photosynthetic pigments (Jørgensen and Des Marais 1988; Kühl and Jørgensen 1992b; Lassen et al. 1992; Kühl et al. 1994). Light scattering can cause locally increased light intensities near the mat surface (e.g. Jørgensen and Des Marais 1988). Increasing surface irradiance increases light penetration and activates photosynthesis in deeper, light-limited parts of the mat, resulting in a deepening of the photic zone. However, many cyanobacteria are able to migrate within the mat and can thus position themselves at depths where favorable light conditions prevail (Castenholz et al. 1991; Garcia-Pichel et al. 1994; Kruschel and Castenholz 1998), including upward migration towards the mat surface at low irradiances and downward migration at high inhibitory irradiances. Furthermore, the zonation and activity of aerobic heterotrophic organisms may also influence the photosynthetic response by alleviating inorganic carbon limitation at high photosynthetic rates (Canfield and Des Marais 1993; Kühl et al. 1996). The P versus E_d curve thus represents the depth-integrated response of the phototrophic community to increasing irradiances, including migration events, light-intensity-induced changes of photosynthetic activity, increases in the thickness of the photic zone and changes of photosynthetic activity in response to varying chemical gradients and heterotrophic activities.

The initial slope, α, of the P versus E_d curve is determined by light-harvesting efficiency and photosynthetic energy conversion efficiency (Henley 1993). Temperature can affect α, since both temperature-independent (photochemical reactions, light absorption, excitation energy transfer) and temperature-sensitive processes (photophosphorylation, electron transport, plastoquinone diffusion) are associated with photosynthesis (Raven and Geider 1988; Davison 1991). Above a certain irradiance, E_k, photosynthesis starts to saturate and approaches a maximal photosynthesis rate, P_m. The light-saturated photosynthetic rate is primarily limited by carbon metabolism, including enzymatic reactions, diffusion and transport processes, and is thus inherently sensitive to temperature (Davison 1991; Henley 1993).

In the Solar Lake mat, maximal photosynthesis at light saturation, P_m, increased with temperature (Fig. 7), indicating that temperature stimulated processes involved in carbon assimilation. The initial slope of the P versus E_d curves and E_k did not show a clear trend with temperature. The temperature optimum of light-saturated photosynthesis was apparently above the in situ temperature of 33 °C (Fig. 9). Rasmussen et al. (1983) found that in situ temperatures were below the experimental optimum temperature for potential photosynthesis in a coastal sediment.

No significant reduction of gross photosynthesis occurred at high irradiances above 626 µmol photons m^{-2} s^{-1} (Fig. 7). The phototrophic community thus

seemed to be high light adapted. Revsbech et al. (1983) did not detect an overall photoinhibition, i.e. a reduction of gross photosynthesis, in a Solar Lake mat with 1670 μmol photons m^{-2} s^{-1} of sunlight. In our study, volumetric gross photosynthetic rates at the mat surface decreased at high irradiances (Fig. 6), indicating a partial photoinhibition of the phototrophic community in the surface layer of the mat (see also Kühl et al. 1997). Whether this reduction was caused only by photoinhibition can, however, not be judged since motile phototrophs can avoid photoinhibitory conditions by downward migration into the mat (Bebout and Garcia-Pichel 1995). Migration could be assumed by the increasing depth of the maximal volumetric gross photosynthesis rate of the subsurface photosynthesis peak at high irradiances (Fig. 6). The reduced rates in the surface layer were apparently compensated by the broadening of the photic zone and increasing rates in deeper layers in response to increased light penetration.

Except at 54 μmol photons m^{-2} s^{-1}, P_g was stimulated by increasing temperatures at each light condition (Fig. 9), indicating that gross photosynthesis was also sensitive to temperature at subsaturating irradiances. At 54 μmol photons m^{-2} s^{-1}, P_g and the thickness of the photic zone strongly decreased at 40 °C (Figs. 5, 9), which could be explained if cyanobacteria switched to an alternative mode of metabolism. Oxygen was almost completely consumed within the photic zone of the mat, and the oxic–anoxic interface was close to the lower boundary of the photic zone (Fig. 5). Temperature-enhanced sulfide production (Skyring et al. 1983; Canfield and Des Marais 1991, 1993; Jørgensen 1994; Wieland and Kühl 2000) could have led to a penetration of sulfide into the cyanobacterial layer of the mat at 40 °C. Thus, the reduction of the (oxygenic) photic zone, and probably also the reduction of gross photosynthesis, could have been due to cyanobacterial anoxygenic photosynthesis (Garlick et al. 1977; Cohen et al. 1986; Jørgensen et al. 1986; de Wit and van Gemerden 1987) or sulfide-inhibition of oxygenic photosynthesis driven by an increased sulfide availability at elevated temperatures. We can also not exclude that some oxygenic gross photosynthesis occurred in the apparent anoxic layer, where photosynthetically produced O_2 was immediately consumed and, therefore, not measurable with O_2 microelectrodes (see also Castenholz et al. 1991).

Net photosynthesis and the total O_2 flux out of the photic zone showed, except at 40 °C, a decreasing trend at irradiances above 626 μmol photons m^{-2} s^{-1} (Fig. 7), indicating an increasing internal O_2 cycling within the mat (see also below). At the compensation irradiance, E_c, gross photosynthesis is balanced by O_2 consumption and thus no net O_2 exchange occurs across the mat–water interface. The compensation irradiance increased with temperature, as O_2 consumption was strongly increased relative to gross photosynthesis. Consequently, higher irradiances were required to turn the mat into a net autotrophic community at elevated temperatures. Increasing compensation irradiances with temperature were also found for the brown alga *Laminaria saccharina* (Davison 1991), and for a temperate hypersaline microbial mat from the Ebro Delta, Spain (E.H.G. Epping and M. Kühl, unpublished results).

Regulation of oxygen consumption by irradiance and temperature

Total O_2 consumption in the mat increased with irradiance. Only at 40 °C did R_{light} decrease at irradiances above 626 μmol photons m^{-2} s^{-1} (Fig. 7). In the light, O_2 consumption occurs both in the photic and in the aphotic zone of the mat. In the aphotic zone of the mat, O_2 was consumed by aerobic respiration and sulfide oxidation. Oxygen consumption in the aphotic zone, R_{aphot}, did not significantly change with irradiance (Fig. 7) and was apparently not directly controlled by photosynthesis (Fig. 8). At 40 °C, R_{aphot} was controlled at low irradiances by the rates of O_2 consumption in the photic zone, and, since the latter were controlled by photosynthesis, R_{aphot} also showed an indirect initial increase with gross photosynthesis (Fig. 8). Enhanced aerobic sulfide oxidation due to temperature-enhanced sulfide production could have caused the significant reduction of the aphotic zone observed at 40 °C (see also Wieland and Kühl 2000).

In the photic zone, both heterotrophic and phototrophic microorganisms can participate in O_2 consumption. Oxygen-consuming processes associated with phototrophic organisms include pseudocyclic electron transport (Mehler reaction), respiration and photorespiration. In the Mehler reaction, O_2 instead of $NADP^+$ is the terminal electron acceptor for (non-cyclic) photosynthetic electron transport, leading to the formation of hydrogen peroxide (Beardall and Raven 1990). In cyanobacteria, O_2 consumption due to the Mehler reaction can increase significantly at high irradiances, where carbon assimilation becomes saturated and thus $NADP^+$ becomes limited relative to the rate of non-cyclic photosynthetic electron transport (Kana 1992). An increased O_2 consumption due to the Mehler reaction can also occur during, e.g., active transport of dissolved inorganic carbon (Miller et al. 1988). However, only if the produced H_2O_2 is not or at least not completely detoxified by catalase, a net O_2 consumption due to the Mehler reaction would occur (Beardall and Raven 1990). Since catalase activity is inhibited by light (Butow et al. 1994), it seems likely that O_2 consumption due to the Mehler reaction could have occurred in the light-incubated mat at high irradiances.

Photorespiration, i.e. O_2 consumption due to the oxygenase activity of ribulose-1,5-bisphosphate carboxylase oxygenase (Beardall and Raven 1990), is thought to be suppressed in cyanobacteria due to their efficient inorganic carbon concentrating mechanisms (Colman 1989). Some marine diatoms can also use bicarbonate (which is converted to CO_2) as an inorganic carbon source for photosynthesis (Korb et al. 1997), but

photorespiration was indicated in diatom-dominated freshwater biofilms (Glud et al. 1992) and in an artificially grown diatom biofilm (Jensen and Revsbech 1989). Thus, photorespiration in the Solar Lake microbial mat cannot be completely excluded, especially under conditions in which high O_2 concentrations prevailed in the mat (Fig. 5).

Photosynthate released during photosynthesis by the phototrophic community can serve as substrate for heterotrophic bacteria and therefore stimulate aerobic respiration. In a hot spring cyanobacterial mat, the production and excretion of photosynthate, mainly glycolate, was shown by Bateson and Ward (1988). An uptake and utilization of excreted photosynthate by heterotrophs is also indicated in other communities (Haack and McFeters 1982; Bateson and Ward 1988; Neely and Wetzel 1995). Furthermore, a close coupling of photosynthesis and heterotrophic respiration was suggested for a hypersaline microbial mat (Canfield and Des Marais 1993) and for an epilithic cyanobacterial biofilm (Kühl et al. 1996). Thus, increasing gross photosynthesis could have led to an increasing release of photosynthate, stimulating aerobic respiration in the photic zone of the Solar Lake mat.

Oxygen consumption in the photic zone of the mat, R_{phot}, generally increased with irradiance and temperature (Figs. 7, 9) and was mainly controlled by gross photosynthesis (Fig. 8). However, some additional factors seem to have controlled O_2 consumption in the photic zone at low and high irradiances. R_{phot} (in percent of P_g) and volumetric rates of O_2 consumption in the photic zone decreased at each incubation temperature between 54 and 119 μmol photons m^{-2} s^{-1} (Table 1; Fig. 9). Thus, at 54 μmol photons m^{-2} s^{-1}, R_{phot} must have been stimulated by other processes than gross photosynthesis; especially at 40 °C, where R_{phot} amounted to 187% of P_g (Fig. 9B). Due to the limited O_2 penetration during darkness, cyanobacteria must have switched to an alternative mode of metabolism than aerobic respiration and/or may have migrated towards the mat surface. Fermentation under dark anaerobic conditions has been demonstrated in several cyanobacteria (Oren and Shilo 1979; Heyer et al. 1989; Moezelaar et al. 1996) and in hot spring mats (Nold and Ward 1996). Hence, accumulated fermentation products could have stimulated heterotrophic respiration at 54 μmol photons m^{-2} s^{-1}. Since this effect was restricted to R_{phot}, and the thickness of the photic zone did not increase as E_d (PAR) was increased from 54 to 119 μmol photons m^{-2} s^{-1} at 25 and 33 °C, we speculate that cyanobacteria migrated towards the mat surface during darkness and remained there at low irradiances. Accumulated fermentation products within this zone may have fuelled aerobic respiration when the light was turned on and photosynthesis led to a sufficient O_2 supply.

Also at high irradiance, some additional temperature-sensitive processes must have influenced O_2 consumption in the photic zone. At 33 °C, R_{phot} increased slightly further at high irradiances although photosynthesis was saturated. At 40 °C, R_{phot} decreased at irradiances above 626 μmol photons m^{-2} s^{-1} (Figs. 7,8). Furthermore, R_{phot} decreased at 40 °C as compared to the lower temperatures, which was independent of gross photosynthesis, since P_g increased with temperature (Fig. 9E, F). This excludes a deleterious effect of the combination of elevated temperatures and irradiances, since the phototrophic population should have then also been affected. Regulating mechanisms, e.g. the release of photosynthate, may have changed at high irradiances in response to temperature, but presently we cannot clearly specify a certain mechanism.

Table 1 Volumetric rates of O_2 consumption in the photic zone, R_{phot}, at experimental irradiances and temperatures

E_d (PAR) (μmol photons m^{-2} s^{-1})	R_{phot} (nmol O_2 cm^{-3} s^{-1})		
	25 °C	33 °C	40 °C
54	0.25	0.58	0.97
119	0.14	0.44	0.89
626	0.67	1.07	1.30
1000	0.70	1.13	0.96
2319	0.97	1.15	0.85

Summary and conclusions

In summary, O_2 consumption in the photic zone was coupled to photosynthesis and contributed significantly to the total O_2 consumption of the microbial mat in the light. Such a coupling can be explained via several possible mechanisms, including photorespiration, the Mehler reaction and the turnover of excreted photosynthate for use by heterotrophic organisms. At moderate irradiances, temperature clearly increased the percentage of the photosynthetically produced O_2 which was consumed within the mat. Thus, elevated temperatures increase the light requirement to turn the mat into a net autotrophic community, as estimated from the O_2 budget. We cannot, however, exclude that photosynthetic CO_2 fixation, and thus net primary production may have been underestimated due to the possibility of anoxygenic photosynthesis. The response of photosynthesis demonstrates an adaptation of the phototrophic community to high irradiances and an apparent optimum temperature of photosynthesis slightly above the in situ temperature.

Dark O_2 consumption in hypersaline mats is strongly regulated by the mass transfer constraints imposed by the diffusive boundary layer. Temperature-enhanced sulfate reduction can indirectly lead to a significant enhancement of dark O_2 consumption and O_2 consumption in the aphotic zone of the illuminated mat due to increased sulfide oxidation. Furthermore, temperature-enhanced sulfate reduction can also lead to an increased sulfide flux out of the dark-incubated mat at higher temperatures (Wieland and Kühl 2000) and therefore to

a loss of reduced species. In the light the mass transfer constraints on oxygen availability are alleviated, and we have shown a pronounced coupling of O_2 production and consumption within the photic zone of the illuminated mat. This coupling is stimulated by irradiance as well as by temperature.

Based on our findings on O_2 turnover, we speculate that the carbon turnover is characterized by a similar close coupling between autotrophs and heterotrophs, which is affected significantly by irradiance and temperature. Such a mechanism has important implications for the way photosynthesis rates are estimated. Traditionally, O_2 consumption in dark incubations is assumed representative for O_2 consumption in the light, and gross O_2 production is estimated by summing net O_2 production in the light with dark O_2 consumption (Geider and Osborne 1992). The use of this approach would significantly underestimate gross photosynthesis in microbial mats, where light-stimulated O_2 consumption takes place. Such an underestimation would be even more pronounced at elevated temperature and/or high irradiance.

Acknowledgements We acknowledge the financial support of the Max-Planck-Society and the Red Sea Program on Marine Sciences, Project E: Microbial activities in marine interfaces controlling sediment–water fluxes, financed by the German Ministry of Education and Research (BMBF). M.K. acknowledges the support by the Danish Natural Science Research Council. We thank G. Eickert, A. Eggers and V. Hübner for the construction of the microsensors. The Interuniversity Institute in Eilat (Israel) is thanked for providing laboratory facilities. Y. Cohen is thanked for his hospitality, inspiration, and for arranging the logistics of the Solar Lake field trip. The Egyptian authorities are thanked for allowing us to work at Solar Lake.

References

Amann R, Kühl M (1998) In situ methods for assessment of microorganisms and their activities. Curr Opin Microbiol 1: 352–358

Barranguet C, Kromkamp J, Peene J (1998) Factors controlling primary production and photosynthetic characteristics of intertidal microphytobenthos. Mar Ecol Prog Ser 173: 117–126

Bateson MM, Ward DM (1988) Photoexcretion and fate of glycolate in a hot spring cyanobacterial mat. Appl envirl Microbiol 54: 1738–1743

Beardall J, Raven JA (1990) Pathways and mechanisms of respiration in microalgae. Mar microb Fd Webs 4(1): 7–30

Bebout BM, Garcia-Pichel F (1995) UVB-induced vertical migrations of cyanobacteria in a microbial mat. Appl envirl Microbiol 61(12): 4215–4222

Blanchard GF, Guarini J-M, Richard P, Gros P, Mornet F (1996) Quantifying the short-term temperature effect on light-saturated photosynthesis on intertidal microphytobenthos. Mar Ecol Prog Ser 134: 309–313

Broecker WS, Peng T-H (1974) Gas exchange rates between air and sea. Tellus 26: 21–35

Butow B, Wynne D, Tel-Or E (1994) Response of catalase activity to environmental stress in the freshwater dinoflagellate *Peridinium gatunense*. J Phycol 30: 17–22

Cadée GC, Hegeman J (1974) Primary production of the benthic microflora living on tidal flats in the Dutch Wadden Sea. Neth J Sea Res 8: 260–291

Canfield DE, Des Marais DJ (1991) Aerobic sulfate reduction in microbial mats. Science 251: 1471–1473

Canfield DE, Des Marais DJ (1993) Biogeochemical cycles of carbon, sulfur, and free oxygen in a microbial mat. Geochim cosmochim Acta 57: 3971–3984

Castenholz RW, Jørgensen BB, D'Amelio ED, Bauld J (1991) Photosynthetic and behavioral versatility of the cyanobacterium *Oscillatoria boryana* in a sulfide-rich microbial mat. Fedn eur microbiol Soc (FEMS) Microbiol Ecol 86: 43–58

Cohen Y, Jørgensen BB, Revsbech NP, Poplawski R (1986) Adaptation to hydrogen sulfide of oxygenic and anoxygenic photosynthesis among cyanobacteria. Appl envirl Microbiol 51(2): 398–407

Cohen Y, Krumbein WE, Goldberg M, Shilo M (1977) Solar Lake (Sinai). 1. Physical and chemical limnology. Limnol Oceanogr 22(4): 597–608

Colman B (1989) Photosynthetic carbon assimilation and the suppression of photorespiration in the cyanobacteria. Aquat Bot 34: 211–231

Davison IR (1991) Environmental effects on algal photosynthesis: temperature. J Phycol 27: 2–8

de Wit R, van Gemerden H (1987) Oxidation of sulfide to thiosulfate by *Microcoleus chtonoplastes*. Fedn eur microbiol Soc (FEMS) Microbiol Ecol 45: 7–13

Epping EHG, Jørgensen BB (1996) Light-enhanced oxygen respiration in benthic phototrophic communities. Mar Ecol Prog Ser 139: 193–203

Fenchel T (1998) Formation of laminated cyanobacterial mats in the absence of benthic fauna. Aquat microb Ecol 14: 235–240

Garcia-Pichel F, Mechling M, Castenholz RW (1994) Diel migrations of microorganisms within a benthic, hypersaline mat community. Appl envirl Microbiol 60(5): 1500–1511

Garcia-Pichel F, Nübel U, Muyzer G (1998) The phylogeny of unicellular, extremely halotolerant cyanobacteria. Archs Microbiol 169: 469–482

Garlick S, Oren A, Padan E (1977) Occurrence of facultative anoxygenic photosynthesis among filamentous and unicellular cyanobacteria. J Bact 129(2): 623–629

Geider RJ, Osborne BA (1992) Algal photosynthesis: the measurement of algal gas exchange. Chapman and Hall, New York

Glud RN, Gundersen JK, Revsbech NP, Jørgensen BB (1994) Effects on the benthic diffusive boundary layer imposed by microelectrodes. Limnol Oceanogr 39: 462–467

Glud RN, Ramsing NB, Revsbech NP (1992) Photosynthesis and photosynthesis-coupled respiration in natural biofilms quantified with oxygen microsensors. J Phycol 28: 51–60

Grant J (1986) Sensitivity of benthic community respiration and primary production to changes in temperature and light. Mar Biol 90: 299–306

Haack TK, McFeters GA (1982) Nutritional relationships among microorganisms in an epilithic biofilm community. Microb Ecol 8: 115–126

Henley WJ (1993) Measurement and interpretation of photosynthetic light-response curves in algae in the context of photoinhibition and diel changes. J Phycol 29: 729–739

Heyer H, Stal L, Krumbein WE (1989) Simultaneous heterolactic and acetate fermentation in the marine cyanobacterium *Oscillatoria limosa* incubated anaerobically in the dark. Archs Microbiol 151: 558–564

Isaksen MF, Jørgensen BB (1996) Adaptation of psychrophilic and psychrotrophic sulfate-reducing bacteria to permanently cold marine environments. Appl envirl Microbiol 62(2): 408–414

Jensen J, Revsbech NP (1989) Photosynthesis and respiration of a diatom biofilm cultured in a new gradient growth chamber. Fedn eur microbiol Soc (FEMS) Microbiol Ecol 62: 29–38

Jørgensen BB (1994) Sulfate reduction and thiosulfate transformations in a cyanobacterial mat during a diel oxygen cycle. Fedn eur microbiol Soc (FEMS) Microbiol Ecol 13(4): 303–312

Jørgensen BB, Cohen Y (1977) Solar Lake (Sinai). 5. The sulfur cycle of the benthic cyanobacterial mats. Limnol Oceanogr 22(4): 657–666

Jørgensen BB, Cohen Y, Revsbech NP (1986) Transition from anoxygenic to oxygenic photosynthesis in a *Microcoleus chthonoplastes* cyanobacterial mat. Appl envirl Microbiol 51(2): 408–417

Jørgensen BB, Des Marais DJ (1988) Optical properties of benthic photosynthetic communities: fiber-optic studies of cyanobacterial mats. Limnol Oceanogr 33(1): 99–113

Jørgensen BB, Des Marais DJ (1990) The diffusive boundary layer of sediments: oxygen microgradients over a microbial mat. Limnol Oceanogr 35(6): 1343–1355

Jørgensen BB, Revsbech NP (1985) Diffusive boundary layers and the oxygen uptake of sediments and detritus. Limnol Oceanogr 30(1): 111–122

Jørgensen BB, Revsbech NP, Blackburn TH, Cohen Y (1979) Diurnal cycle of oxygen and sulfide microgradients and microbial photosynthesis in a cyanobacterial mat sediment. Appl envirl Microbiol 38(1): 46–58

Jørgensen BB, Revsbech NP, Cohen Y (1983) Photosynthesis and structure of benthic microbial mats: microelectrode and SEM studies of four cyanobacterial communities. Limnol Oceanogr 28(6): 1075–1093

Kana TM (1992) Relationship between photosynthetic oxygen cycling and carbon assimilation in *Synechococcus* WH7803 (Cyanophyta). J Phycol 28: 304–308

Korb RE, Saville PJ, Johnston AM, Raven JA (1997) Sources of inorganic carbon for photosynthesis by three species of marine diatom. J Phycol 33: 433–440

Krumbein WE, Cohen Y, Shilo M (1977) Solar Lake (Sinai). 4. Stromatolitic cyanobacterial mats. Limnol Oceanogr 22(4): 635–656

Kruschel C, Castenholz RW (1998) The effect of solar UV and visible irradiance on the vertical movements of cyanobacteria in microbial mats of hypersaline waters. Fedn eur microbiol Soc (FEMS) Microbiol Ecol 27: 53–72

Kuenen JG, Jørgensen BB, Revsbech NP (1986) Oxygen microprofiles of trickling filter biofilms. Wat Res 20(12): 1589–1598

Kühl M, Glud RN, Ploug H, Ramsing NB (1996) Microenvironmental control of photosynthesis and photosynthesis-coupled respiration in an epilithic cyanobacterial biofilm. J Phycol 32: 799–812

Kühl M, Jørgensen BB (1992a) Microsensor measurements of sulfate reduction and sulfide oxidation in compact microbial communities of aerobic biofilms. Appl envirl Microbiol 58(4): 1164–1174

Kühl M, Jørgensen BB (1992b) Spectral light measurements in microbenthic phototrophic communities with a fiber-optic microprobe coupled to a sensitive diode array detector. Limnol Oceanogr 37(8): 1813–1823

Kühl M, Lassen C, Jørgensen BB (1994) Optical properties of microbial mats: light measurements with fiber-optic microprobes. In: Stal LJ, Caumette P (eds) Microbial mats: structure, development and environmental significance. NATO ASI Series G. Vol. 35. Springer, Berlin, pp 149–166

Kühl M, Lassen C, Revsbech NP (1997) A simple light meter for measurements of PAR (400 to 700 nm) with fiber-optic microprobes: application for P vs E_0 (PAR) measurements in a microbial mat. Aquat microb Ecol 13: 197–207

Lassen C, Ploug H, Jørgensen BB (1992) Microalgal photosynthesis and spectral scalar irradiance in coastal marine sediments of Limfjorden, Denmark. Limnol Oceanogr 37(4): 760–772

Li Y-H, Gregory S (1974) Diffusion of ions in sea water and in deep-sea sediments. Geochim cosmochim Acta 38: 703–714

Lorenzen J, Glud RN, Revsbech NP (1995) Impact of microsensor-caused changes in diffusive boundary layer thickness on O_2 profiles and photosynthetic rates in benthic communities of microorganisms. Mar Ecol Prog Ser 119: 237–241

Miller AG, Espie GS, Canvin DT (1988) Active transport of inorganic carbon increases the rate of O_2 photoreduction by the cyanobacterium *Synechococcus* UTEX 625. Pl Physiol 88: 6–9

Millero FJ, Poisson A (1981) International one-atmosphere equation of state of seawater. Deep-Sea Res 28: 625–629

Moezelaar R, Bijvank SM, Stal LJ (1996) Fermentation and sulfur reduction in the mat-building cyanobacterium *Microcoleus chthonoplastes*. Appl envirl Microbiol 62(5): 1752–1758

Neely RK, Wetzel RG (1995) Simultaneous use of ^{14}C and ^{3}H to determine autotrophic production and bacterial protein production in periphyton. Microb Ecol 30: 227–237

Nold SC, Ward DM (1996) Photosynthate partitioning and fermentation in hot spring microbial mat communities. Appl envirl Microbiol 62(12): 4598–4607

Oren A, Shilo M (1979) Anaerobic heterotrophic dark metabolism in the cyanobacterium *Oscillatoria limnetica*: sulfur respiration and lactate fermentation. Archs Microbiol 122: 77–84

Rasmussen MB, Henriksen K, Jensen A (1983) Possible causes of temporal fluctuations in primary production of the microphytobenthos in the Danish Wadden Sea. Mar Biol 73: 109–114

Raven JA, Geider RJ (1988) Temperature and algal growth. New Phytol 110: 441–461

Revsbech NP (1989) An oxygen microelectrode with a guard cathode. Limnol Oceanogr 34: 474–478

Revsbech NP, Jørgensen BB (1983) Photosynthesis of benthic microflora measured with high spatial resolution by the oxygen microprofile method: capabilities and limitations of the method. Limnol Oceanogr 28(4): 749–756

Revsbech NP, Jørgensen BB (1986) Microelectrodes: their use in microbial ecology. Adv microb Ecol 9: 293–352

Revsbech NP, Jørgensen BB, Blackburn TH, Cohen Y (1983) Microelectrode studies of the photosynthesis and O_2, H_2S, and pH profiles of a microbial mat. Limnol Oceanogr 28(6): 1062–1074

Revsbech NP, Jørgensen BB, Brix O (1981) Primary production of microalgae in sediments measured by oxygen microprofile, $H^{14}CO_3$-fixation, and oxygen exchange methods. Limnol Oceanogr 26(4): 717–730

Riley JP, Skirrow G (1975) Chemical oceanography. Academic Press, London, p 338

Sherwood JE, Stagnitti F, Kokkinn MJ, Williams WD (1991) Dissolved oxygen concentrations in hypersaline waters. Limnol Oceanogr 36(2): 235–250

Skyring GW, Chambers LA, Bauld J (1983) Sulfate reduction in sediments colonized by cyanobacteria, Spencer Gulf, South Australia. Aust J mar Freshwat Res 34: 359–374

Stal LJ, Caumette P (1994) Microbial mats: structure, development and environmental significance. Springer, Berlin

Thamdrup B, Hansen JW, Jørgensen BB (1998) Temperature dependence of aerobic respiration in a coastal sediment. Fedn eur microbiol Soc (FEMS) Microbiol Ecol 25: 189–200

Ullman WJ, Aller RC (1982) Diffusion coefficients in nearshore marine sediments. Limnol Oceanogr 27(3): 552–556

van Gemerden H (1993) Microbial mats: a joint venture. Mar Geol 113: 3–25

Vogel S (1989) Life in moving fluids. Princeton University Press, Princeton, New Jersey

Webb WL, Newton M, Starr D (1974) Carbon dioxide exchange of *Alnus rubra*: a mathematical model. Oecologia 17: 281–291

Wieland A, Kühl M (2000) Short-term temperature effects on oxygen and sulfide cycling in a hypersaline cyanobacterial mat (Solar Lake, Egypt). Mar Ecol Prog Ser 196: 87–102